IOP Conference Series: Materials Science and Engineering

PAPER • OPEN ACCESS

Modelling of chemical shrinkage evolution with curing degree of a filled epoxy adhesive

To cite this article: T Holst *et al* 2020 *IOP Conf. Ser.: Mater. Sci. Eng.* **942** 012020

IOP Conf. Series: Materials Science and Engineering **942** (2020) 012020 doi:10.1088/1757-899X/942/1/012020

Modelling of chemical shrinkage evolution with curing degree of a filled epoxy adhesive

T Holst[1,2,3], **F Sayer**[1] **and A Antoniou**[1]

[1] Fraunhofer Institute for Wind Energy Systems, Am Seedeich 45, 27572 Bremerhaven, Germany
[2] Institute for Wind Energy Systems, Leibniz University Hanover, Appelstraße 9A, 30167 Hanover, Germany

[3] Corresponding author`s e-mail: tobias.holst@iwes.fraunhofer.de

Abstract. An epoxy adhesive system, commonly used in wind turbine blade manufacturing, is experimentally investigated with respect to its chemical shrinkage behavior to show the shrinkage evolution within rotor blade production related process conditions. Therefore, a new test configuration is set up to record the resulting chemical shrinkage of the adhesive at cross-linking temperatures ranging from 20°C to 90°C. The respective conversion evolution is simulated under several temperature conditions through a curing kinetics model. This is generated with state of the art formulations, implementing test results from a differential scanning calorimeter (DSC). Moreover, the transformation of the curing degree to the corresponding glass transition temperature (T_g) is performed through an experimentally based Di-Benedetto curve-fitting. By the combination of curing kinetics and chemical shrinkage test data, a model for the temperature and conversion dependant chemical shrinkage evolution during cure is developed. This is applied to a realistic curing cycle for adhesive materials in rotor blade production.

1. Introduction

To meet today's requirements in the wind energy market, wind turbine rotor blades must embody improved mechanical performance and reliability [1, 2]. Chemical shrinkage effects during curing of bond lines, are one of the main drivers for induced residual stress states after manufacturing, which can influence the mechanical performance of the adhesive by promoting crack initiations [3, 4]. It is therefore important to understand the process related evolution of chemical shrinkage. Material specific shrinkage values are often not known, since the characterization is complicated [3, 5–7].

The above-mentioned chemical shrinkage effect can be explained with decreasing mean gaps within the macromolecule structure in progression of cross-linking [5]. Therefore the adhesive shrinkage behavior is highly related to the chemical structure and additives [3, 5, 6]. For the characterization, isothermal measurement conditions are essential to decouple chemical from thermal shrinkage effects [7]. Previous research showed that the measurement technique according to the principle of Archimedes' can deliver proper test results with accurate resolution [5, 8–10].

A widely common assumption, found in literature, is a linear connection between degree of cure and chemical shrinkage values [3, 5, 8, 11]. In addition, some authors assume a nonlinear shrinkage

evolution, which is influenced by gelation and viftrification [9, 12]. Therefore the knowledge of the curing kinetic behavior is of importance to display the relation towards conversion.

Curing kinetics are describing the curing progress respectively to ambient curing conditions. Cure dependent characteristics like reaction heat can be implemented into model environments [13, 14]. To model the curing behavior of epoxy resins with amine hardeners, a common, state of the art approach, found in literature, is introduced by Kamal-Sourour [15]. The named model is an extension of a simple autocatalytic curing correlation, combined with a simple n^{th}-order-reaction [16, 17]. Acceleration effects of the reaction rate due to intermediate reaction products are characteristic for autocatalytic reaction types. More complex curing kinetic models are available. With additional mathematical functions, the diffusion controlled curing process, induced by vitrification effects, can be taken into account [17–19]. Often these models require the conversion dependent development of the glass transition temperature (T_g) [19]. This relationship can be expressed by the Di-Benedetto-equation and is common in literature [19–22].

This scientific work contributes to the characterization of new material-specific properties during cure. For the selected adhesive system the curing kinetic behavior is determined and a model of the chemical shrinkage evolution is generated with new test methods. The shrinkage model is applied with regard to application related curing conditions.

2. Experimental setup

For analyzing the chemical shrinkage, a two-step experimental characterization method was chosen. At first, the curing kinetic behavior of the adhesive system was examined, using DSC. Subsequently, the time-dependent chemical shrinkage was measured in a temperature range from 20 °C to 90 °C and then compared with the time-dependent conversion data.

2.1. Material

Epikote MGS BPR 135 G3 resin in combination with *Epikure MGS BPH 137G* curing agent from Hexion was used in the following research [23]. The selected material is an industry standard epoxy adhesive system for rotor blade production.

2.2. Determination of experimental data for curing kinetic modelling

A *Netzsch DSC 204 F1* was used for the curing characterization procedure. Four different temperature stages (60 °C, 80 °C, 100 °C and 120 °C) were chosen to track the curing behavior under isothermal conditions. Three specimens were tested at each temperature level. The lower limit of the temperature range is defined by the sensitivity of the heat flow sensor, whereas the upper limit is set by exothermal effects of the specimen itself.

Before starting the measurement, uncured adhesive specimen, embedded in aluminum pans, were put in the preheated measuring chamber to achieve immediately the desired temperature level, followed directly by a start of the measurement. It is assumed that during the very short heat-up-phase (below 10 s), the specimen does not undergo any curing. During the described isothermal stages the time dependent heat flow $h_{iso}(t)$ of the curing reaction was monitored until the reaction came to a standstill at t_{end}. Whereas $H_{iso}(t)$ is the integral of the heat flow curve from the start of the reaction at t_0 to the present time t.

After the isothermal stage, a temperature-modulated dynamic ramp from 0 °C to 250 °C was applied on the specimens to track the heat flow during post curing to full cure, H_{res}. The modulated ramp function was used to generate a smooth base line level and isolate effects due to glass transition. A heating ramp of 3 K/min, an amplitude of 0.5 K and a period of 60 s was set for the DSC-measurement.

The development of the degree of cure $p(t)$ was then calculated by correlating the time-depending amount of heat energy during isothermal cure $H_{iso}(t)$ to the total amount of heat release H_{tot},

$$p(t) = \frac{H_{iso}(t)}{H_{tot}} = \frac{\int_0^t h_{iso}(t)dt}{\int_0^{t_{end}} h_{iso}(t)dt + H_{res}} \quad (1)$$

The Di-Benedetto relation, describing the conversion dependent glass transition temperature, was derived by determining the glass transition temperatures of uncured, partially cured and fully cured samples. The midpoint method according to DIN EN ISO 11357-2 with 20 K/min heating ramp was used for the analysis.

2.3. Chemical shrinkage test rig

The design of the test rig for measuring the chemical shrinkage effect is based on the Archimedean Principle. The used shrinkage test rig consists of a tempered oil bath, which contains the measuring chamber, filled with silicone oil, see Figure 1. To avoid any chemical reactions with the adhesive specimen, the silicone oil has inert chemical properties. The specimen holder, especially developed for pasty adhesive materials, is hanged in the silicon oil below a precision scale. For temperature documentation, each oil bath owns a temperature sensor.

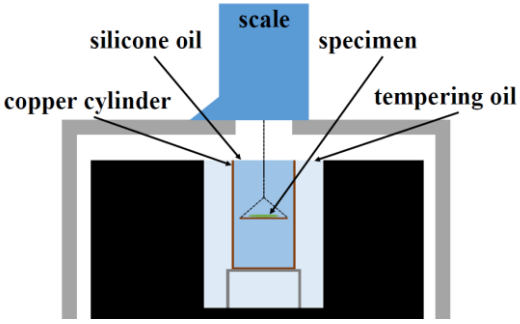

Figure 1. Schematic construction of chemical shrinkage test rig.

Knowing the weight of the specimen in air m_{air} and the density of the silicone oil $\rho_{oil}(T)$ at certain temperatures T, the volume of the specimen $V(t)$ in theory, can be determined any time t by its weight in oil $m_{oil}(t)$, based on the Principle of Archimedes'.

$$V(t) = \frac{m_{air} - m_{oil}(t)}{\rho_{oil}(T)} \tag{2}$$

In the measurement procedure the weight value of the scale measurement $m_S(t)$ in oil consists of the sample and the sample holder. To isolate the effect of the sample holder, its weight in oil $m_{Hoil}(T)$ must be known at respective temperatures T. The volume of the specimen can then be calculated.

$$V(t) = \frac{m_{air} - (m_S(t) - m_{Hoil}(T))}{\rho_{oil}(T)} \tag{3}$$

By comparing the change of the specimen volume $\Delta V(t)$ during cure to the starting volume $V(t_0)$, the chemical shrinkage value S can be calculated.

$$S(t) = \frac{\Delta V(t)}{V(t_0)} = \frac{V(t_0) - V(t)}{V(t_0)} \tag{4}$$

Three specimen were tested each at eight curing temperature levels in a range from 20 °C to 90 °C. For monitoring the specimen temperature, in order to detect unwanted exothermal effects, an additional measurement was made for each temperature with identical specimen geometries without tracking the scale data. Otherwise, the measurement would be highly affected by the temperature sensor due to the high sensitivity of the measuring configuration.

3. Model results and discussion

At first, the modelling results of the curing kinetics are presented. These are then combined with the chemical shrinkage data to show and model the relation with conversion.

3.1. Curing kinetics

The modelling of the curing kinetics was performed by a parameter fit of the model data to the experimental data by using a least square method in a dp/dt-p-diagram. The mean p-values of the three performed measurements at each temperature have been used as the data basis for the fit, see Figure 2. At first a Kamal-Sourour model approach was used, Equation (5). The temperature dependent reaction rate constants k_1 and k_2 can be calculated with the Arrhenius correlation, Equation (7).

The parameter fit leads to a reaction rate constant k_1 (A_1=2075841 1/s and E_{a1}=555214 J/mol) which tends towards zero at variable curing temperatures T. Therefore the model approach can be simplified to an autocatalytic model with only one remaining reaction rate constant k_2, Equation (6). The updated model parameters are shown below in Table 1. Since the model environment is implemented in further calculations, a simpler model approach is preferred to reduce the overall calculation effort.

$$\frac{dp}{dt} = (k_1 + k_2 p^m)(1-p)^n \tag{5}$$

$$\frac{dp}{dt} = k_2 p^m (1-p)^n \tag{6}$$

$$k_{1,2} = A_{1,2} * e^{\frac{-E_a 1,2}{RT}} \tag{7}$$

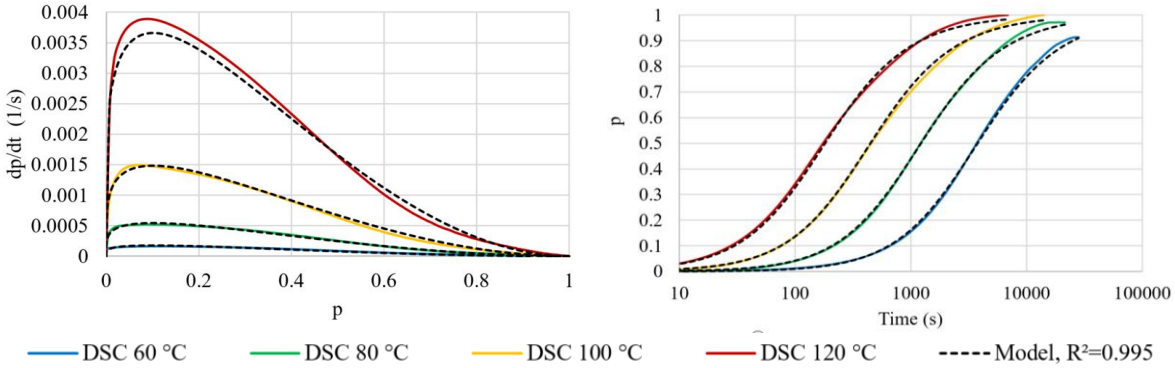

Figure 2. Least square fit of autocatalytic curing model parameters, mean values of measured data.

Table 1. Determined parameters for autocatalytic curing model.

A_2 (1/s)	E_{a2} (J/mol)	m	n
153965	55055	0.22	1.95

The development of the glass transition temperature is described with the Di-Benedetto-relation, Equation (8). The parameters T_{g0} and $T_{g\infty}$ were determined with glass transition temperature measurements of uncured and fully cured DSC-samples (DIN EN ISO 11357-2 midpoint method, 20 K/min). The Di-Benedetto-parameter λ can be calculated by using a least square data fit as seen in Figure 3. Determined parameters for the Di-Benedetto-equation are listed in Table 2.

$$\frac{T_g - T_{g0}}{T_{g\infty} - T_{g0}} = \frac{\lambda p}{1-(1-\lambda)p} \tag{8}$$

Table 2. Determined parameters for Di-Benedetto relation.

T_{g0} (°C)	$T_{g\infty}$ (°C)	λ
-40.9	90.9	0.377

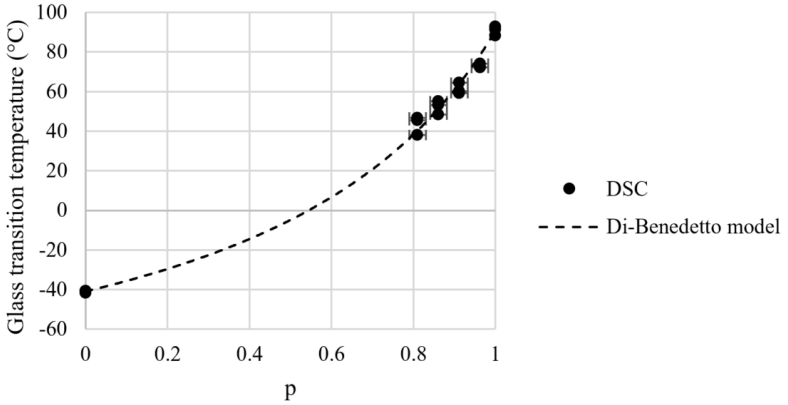

Figure 3. Least square fit of Di-Benedetto model data.
*Note: some error bars not visible, as deviations are very small

By looking at Equation (6) the mathematical forecast for the development of the conversion is reaching full cure after a certain amount of time at arbitrary temperatures. Under real conditions at lower curing temperatures, the curing reaction comes to a standstill because of vitrification effects. Taking this into account an additional simple condition can be implemented into the curing model environment. This condition includes a stop criterion when the rising glass transition temperature of the curing system is more than a certain temperature range T_S above the current curing temperature, Equation (9).

$$\frac{dp}{dt} = \begin{cases} k_2 p^m (1-p)^n \\ 0 \end{cases} \quad for \quad \begin{matrix} T_g(p) - T \leq T_S \\ T_g(p) - T > T_S \end{matrix} \tag{9}$$

To find a suitable value for T_S, adhesive specimens, equipped with temperature sensors, were cured in an oven under variable curing cycles reaching from 40 °C to 100 °C, followed by analyzing the glass transition temperatures $T_g\,(DSC)$ afterwards with DSC-measurements (DIN EN ISO 11357-2 midpoint method, 20 K/min). According to the total square deviation, T_S=30 °C yields the highest fit between model prediction and measured data, Table 3.

Table 3. Adaptation of stop criterion for curing kinetics model.

			Model forecast			
Hold time (*h*)	Oven temperature (°C)	T_g (DSC) (°C)	*Ts=20 °C* (°C)	*Ts=25 °C* (°C)	*Ts=30 °C* (°C)	*Ts=35 °C* (°C)
48	40	70.4	60.1	65.1	69.9	74.8
24	50	73.5	70.0	74.3	74.8	75.2
12	60	74.2	73.9	74.5	75.0	75.4
6	70	77.4	73.9	74.5	75.0	75.4
3	80	77.9	72.9	73.5	73.5	74.6
1.5	90	77.7	73.0	73.6	73.6	74.7
0.75	100	76.3	72.4	72.6	72.6	72.7
	Total square deviation (°C²):		**192.1**	**86.2**	**57.3**	**61.3**

The model environment of the curing kinetics gives a good agreement with the measurement data by using a modified autocatalytic model with an implemented stop criterion, which simplifies the effect of diffusion controlled reaction progress. More complex curing models, containing diffusion controlled elements, have also been analyzed and deliver similar results.

3.2. Chemical shrinkage

The following diagram shows the evaluated mean shrinkage values at variable temperature levels plotted against conversion, Figure 4. Visible is a linear connection between shrinkage and degree of cure. Several studies in literature, like Holst [7] observed the same behavior. Minor variations from the linear relation can be explained with uncertainties of the curing kinetics model due to slightly exothermal behavior and vitrification effects at high degrees of cure.

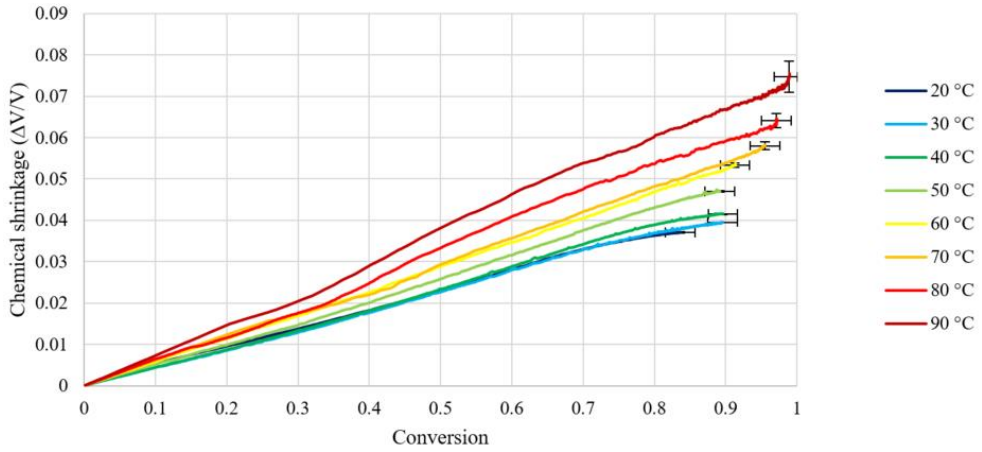

Figure 4. Mean values of observed chemical shrinkage with conversion and temperature. *Note: some error bars not visible, as deviations are very small

Furthermore, the gradients are dependent on the curing temperature. Therefore, at similar degrees of cure, a range of different chemical shrinkage values can be observed. An increasing trend is recognizable with higher curing temperatures. Blumenstock [10] obtained similar results. Here this effect is explained with different amounts of free volumes which are being frozen within the curing process at different temperature levels. This can be described closer with detailed information of the occurring thermal shrinkage effects during cure. Since these details are not known, a simple model approach for describing the temperature dependent chemical shrinkage of the adhesive was chosen.

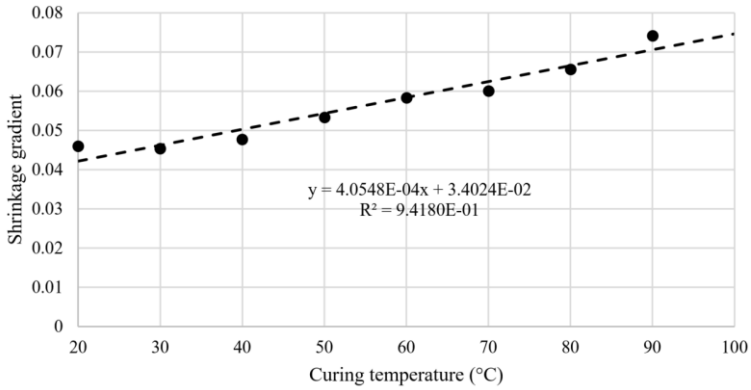

Figure 5. Model approach for chemical shrinkage gradients with temperature dependency.

By plotting the respective straight line gradients of the shrinkage measurements with their corresponding curing temperatures, a linear relationship is visible, Figure 5.

Table 4. Determined parameters for shrinkage gradient modelling.

a (1/°C)	b
$4.0548*10^{-4}$	$3.4024*10^{-2}$

The parameters of the linear regression a and b, Table 4, can be used to derive an equation for predicting the chemical shrinkage development S with conversion p and ambient curing temperature θ in °C.

$$S = p(a\theta + b) \tag{10}$$

4. Conclusions

The developed models for curing and chemical shrinkage forecast can be used for an application towards a chosen representative curing cycle for the adhesive material in rotor blade production, see Figure 6.

It can be seen that the displayed curing cycle initially remains at a low temperature for the application of the adhesive at 40 °C. After the subsequent joining process, the temperature is increased to accelerate the curing of the adhesive material. At higher temperatures, the reaction rate of the exothermic curing reaction has the effect of a temperature overshoot. In this phase most of the curing progress and also most of the chemical shrinkage take place. After this, a temperature level of 80 °C is maintained constant to achieve the desired degree of cure. At the end of the curing cycle it can be seen that a glass transition temperature of approximately 80 °C has been reached and a chemical volume shrinkage of 7% has taken place in the adhesive material.

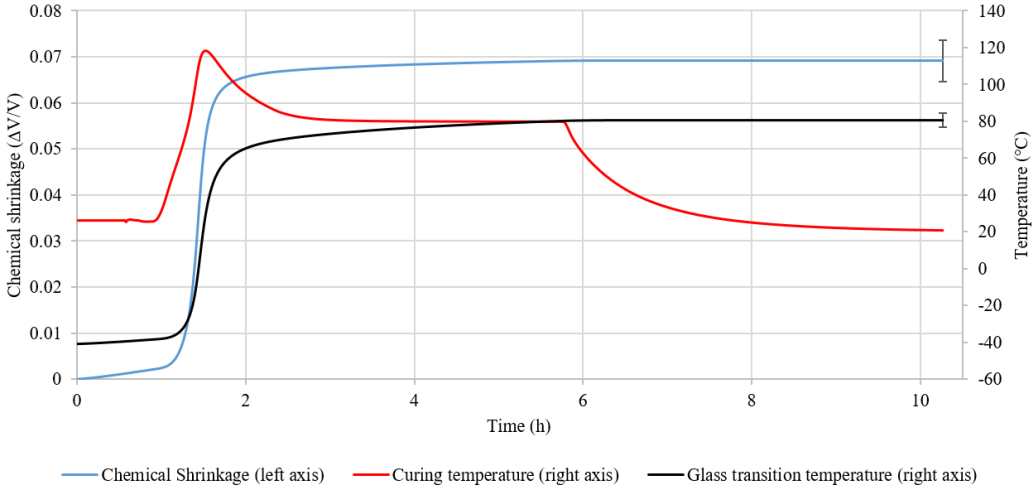

Figure 6. Application of chemical shrinkage- and curing model to a curing cycle.

These illustrations of the mechanisms during the curing process are one of the bases for understanding the development of residual stresses in bond lines during rotor blade manufacturing. In future research works, material specific values for the related thermal shrinkage behavior are of great importance. Besides the knowledge of specific values for further model development towards residual stress prediction, the thermal shrinkage data can also be used to formulate an alternative model approach for describing the temperature dependent chemical shrinkage according to the frozen volume theory. This will contribute to further validate the presented work.

Acknowledgments
We acknowledge the support provided by the German Federal Ministry for Economic Affairs and Energy (BMWi) within the Smart Blades 2.0 project (0324032B/C).

References

[1] Toft H S and Sørensen J D 2011 Reliability-based design of wind turbine blades. *Structural Safety* **33** 333–42.
[2] Hayman B, Wedel-Heinen J, and Brøndsted P 2008 Materials challenges in present and future wind energy. *MRS Bull.* **33** 343–53.
[3] Schümann J-P 2018. *Zur zeit-, temperatur- und umsatzabhängigen Entwicklung polymerphysikalischer Vernetzungsschwindung aminisch vernetzender Epoxide* Dissertation. Technical University of Clausthal, Clausthal.
[4] Jørgensen J B, Sørensen B F, and Kildegaard C 2019 The effect of residual stresses on the formation of transverse cracks in adhesive joints for wind turbine blades. *International Journal of Solids and Structures* **163** 139–56.
[5] Holst M 2001. *Reaktionsschwindung von Epoxidharz-Systemen* Dissertation. Technical University of Darmstadt, Darmstadt.
[6] Haider M, Hubert P, and Lessard L 2007 Cure shrinkage characterization and modeling of a polyester resin containing low profile additives. *Composites Part A: Applied Science and Manufacturing* **38** 994–1009.
[7] Holst M, Schänzlin K, Wenzel M, Xu J, Lellinger D, and Alig I 2005 Time-resolved method for the measurement of volume changes during polymerization. *J. Polym. Sci. B Polym. Phys.* **43** 2314–25.
[8] Khoun L and Hubert P 2010 Cure shrinkage characterization of an epoxy resin system by two in situ measurement methods. *Polym Compos* **31** 1603–10.
[9] Li C, Potter K, Wisnom M R, and Stringer G 2004 In-situ measurement of chemical shrinkage of MY750 epoxy resin by a novel gravimetric method. *Composites Science and Technology* **64** 55–64.
[10] Blumenstock T 2003. *Analyse der Eigenspannungen während der Aushärtung von Epoxidharzmassen* Dissertation. University of Stuttgart, Stuttgart.
[11] Billotte C, Bernard F M, and Ruiz E 2013 Chemical shrinkage and thermomechanical characterization of an epoxy resin during cure by a novel in situ measurement method. *European Polymer Journal* **49** 3548–60.
[12] Wenzel M 2005. *Spannungsbildung und Relaxationsverhalten bei der Aushärtung von Epoxidharzen* Dissertation. Technical University of Darmstadt, Darmstadt.
[13] Hardis R, Jessop J LP, Peters F E, and Kessler M R 2013 Cure kinetics characterization and monitoring of an epoxy resin using DSC, Raman spectroscopy, and DEA. *Composites Part A: Applied Science and Manufacturing* **49** 100–8.
[14] Deutsches Institut für Normung e.V. 2014 DIN EN ISO 11357-5 Plastics - Differential scanning calorimetry (DSC) - Part 5: Determination of characteristic reaction-curve temperatures and times, enthalpy of reaction and degree of conversion.
[15] Sourour S and Kamal M R 1976 Differential scanning calorimetry of epoxy cure: isothermal cure kinetics. *Thermochimica Acta* **14** 41–59.
[16] Yousefi A, Lafleur P G, and Gauvin R 1997 Kinetic studies of thermoset cure reactions: A review. *Polym. Compos.* **18** 157–68.
[17] Karkanas P I, Partridge I K, and Attwood D 1996 Modelling the cure of a commercial epoxy resin for applications in resin transfer moulding. *Polym. Int.* **41** 183–91.
[18] Cole K C, Hechler J-J, and Noel D 1991 A new approach to modeling the cure kinetics of epoxy/amine thermosetting resins. *Macromolecules* **24** 3098–110.
[19] Javdanitehran M, Berg D C, Duemichen E, and Ziegmann G 2016 An iterative approach for isothermal curing kinetics modelling of an epoxy resin system. *Thermochimica Acta* **623** 72–9.

[20] DiBenedetto A T 1987 Prediction of the glass transition temperature of polymers: A model based on the principle of corresponding states. *J. Polym. Sci. B Polym. Phys.* **25** 1949–69.
[21] Yu H, Mhaisalkar S G, Wong E H, and Khoo G Y 2006 Time–temperature transformation (TTT) cure diagram of a fast cure non-conductive adhesive. *Thin Solid Films* **504** 331–5.
[22] O'Brien D J and White S R 2003 Cure kinetics, gelation, and glass transition of a bisphenol F epoxide. *Polym. Eng. Sci.* **43** 863–74.
[23] Hexion. *Technical data sheet*. *EP-Klebeharz Epikote BPR 135G + Epikure BPH 134G-137GF*. Retrieved May 19, 2020 from https://www.hexion.com/en-US/product/--archive--epikote-resin-mgs-bpr-135g-series-and-epikure-curing-agent-mgs-bph-134g-137gf.